
ORDER, DISORDER, AND PHASE TRANSITION
IN CONDENSED SYSTEM

Interaction of a Magnetic Vortex with Magnetic Anisotropy Nonuniformity

V. A. Orlov^{a,b,*}, G. S. Patrin^{a,b}, and I. N. Orlova^c

^a Siberian Federal University, Krasnoyarsk, 660041 Russia

^b Kirensky Institute of Physics, Federal Research Center “Krasnoyarsk Scientific Center,”
Siberian Branch, Russian Academy of Sciences, Krasnoyarsk, 660036 Russia

^c Astaf'ev Krasnoyarsk State Pedagogical University, Krasnoyarsk, 660049 Russia

*e-mail: vaorlov@sfu-kras.ru

Received February 19, 2020; revised March 16, 2020; accepted March 18, 2020

Abstract—The problem of propagation of a magnetic inhomogeneity in the form of a magnetic vortex near a defect simulated by a crystallite with uniaxial anisotropy has been solved theoretically. The defect (crystallite) is implanted into a homogeneous 2D ferromagnetic matrix. Apart from the anisotropy energy, the term responsible for the existence of a centrosymmetric potential is included into the total energy. For calculations, we have used the method of collective variables (Thiele equation). We have considered the variants of bidirectional and unidirectional anisotropy of the crystallite. Analysis of the equations of motion for different directions of the anisotropy axis of the implanted defect has revealed the variety in the behavior of the vortex core as a quasiparticle. The vortex core can be trapped by the defect with equilibrium position of the vortex at rest directly on the crystallite or during its motion at a certain distance from it. It is shown that for a small damping parameter and in the case when the defect anisotropy axis lies in the plane of the magnet, the vortex moves so as if its core experiences the action of the repulsive axially symmetric potential.

DOI: 10.1134/S1063776120090071

1. INTRODUCTION

In recent years, the interest in experimental and theoretical investigation of magnets with the vortex structure of magnetization has not subsided. Keen interest in such materials is associated with prospects of their application in various spintronics devices [1–4]. Topological inhomogeneities in the magnetization (such as magnetic vortices, skyrmions, and domain walls with a vortex structure) exhibit unique properties, which render them good candidates for data and memory storage devices. Analysis of magnetic vortices is of special importance in the investigation of superconductors (see, for example, [5]).

The magnetic vortex dynamics in static and varying fields in nanosize magnets of various geometrical shapes and their aggregates has been studied quite comprehensively [6–12]. Many properties of vortex formations have been predicted and verified experimentally. The method of collective variables proved to be very productive in describing the evolution of magnetization in magnets with a vortex structure. In this method, the description of motion of a magnetic vortex is reduced to solving the equation for a quasiparticle, the properties of which are determined by magnetic parameters of the vortex. In this case, it is convenient to choose the coordinate of the vortex center and

its velocity as collective variables. The equation of motion in this case is non-Newtonian.

It is convenient to define the magnetic state of a vortex (a skyrmion) by two parameters: polarity p of the core and chirality q . The vortex core is its central part of a quite small size (about 10 nm) with a clearly manifested nonuniformity of the magnetization. Because of the competition between the exchange energy and the demagnetization energy, the magnetization at the core center is perpendicular to the plane of the vortex and can coincide with the direction of the preferred z axis ($p > 0$) or be opposite to it ($p < 0$). The orientation of the magnetization in the vortex “skirt” (“tail”) can coincide with a right-hand screw relative to the z axis (positive chirality, $q > 0$) or be opposite to it ($q < 0$).

Most theoretical publications with analytic calculations and computer simulation are devoted to analysis of static and dynamic properties of magnetic vortices in materials without magnetic nonuniformities in exchange, anisotropy, etc.; i.e., models without defects are considered. At the same time, spatial fluctuations of magnetic parameters exist in real materials with a vortex structure and affect the motion of magnetic vortices. A large number of theoretical publications are devoted to accounting for the effect of various types of inhomogeneities on the properties of mag-

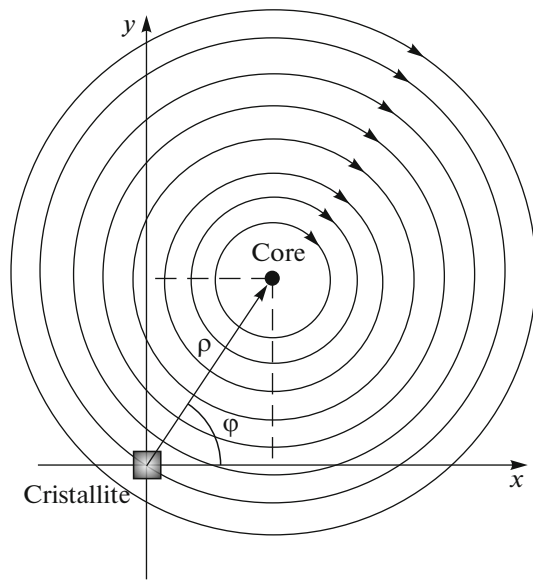


Fig. 1. Model of interaction of the vortex magnetization with the magnetic anisotropy nonuniformity.

netic vortices. For example, in [13–16], a point defect was simulated by the nonuniformity of the magnetic anisotropy constant; for this reason, a model potential with axial symmetry was used. In [17, 18], a point inhomogeneity of the atomic size was simulated by the variation of the exchange constant. Not only point defects, but also extended defects [9, 13] and even inhomogeneity in the form of holes [19] were considered in the literature. Publications [17, 20, 21] in which the authors took into account a large number of factors simulating the nonuniformity of magnetic parameters are especially worth mentioning. In the whole, the results of all investigations indicated that the consequences of the interaction of a magnetic vortex (as well as a skyrmion) with a defect are extremely diversified. The core can be trapped by the defect or can be reflected from it.

The trajectory of the core near a defect can be intricate and often cannot be described analytically. For this reason, computer simulation is often used for obtaining practically feasible results [22–25]. Simulation makes it possible to predict the influence of the defect field on the mobility of vortices and skyrmions and on the manifestations of the Hall effect [26–28]. In [29, 30], simulation was employed for detecting a peculiar behavior of a moving skyrmion crossing a linear defect (the trajectory is bent, resembling the refraction of light). The effect of surface roughness on the mobility of skyrmions was considered in [31], and the possibility in principle to control the potential produced by a defect with the help of fields was demonstrated in [4, 32].

We must also mention important experimental results of observation of vortices and/or skyrmions, which were also reported in the literature. In [33–35],

the authors demonstrated scenarios of pinning of vortices (or skyrmions) at crystal structure defects. The behavior of vortex structures in a magnet with surface inhomogeneities was analyzed in [36], and the field mechanism of controlling the extent of influence of defects on the motion of skyrmions was demonstrated in [37].

In this study, we analyze theoretically of the influence of a defect in the form of an implanted crystallite with a magnetic anisotropy differing from that of the main matrix on the behavior of a magnetic vortex. The nonuniformity of the anisotropy field is ensured by not the variation of the anisotropy constant as in the aforementioned publications, but of the direction of the local anisotropy axis. In this case, the defect can produce a potential without the axial symmetry, and we can expect interesting effects associated with the absence of such symmetry.

2. EQUATION OF MOTION OF THE MAGNETIZATION IN THE VICINITY OF A DEFECT

Let us consider the following model of interaction of the magnetization of a vortex with a nonuniformity. A crystallite of a small volume V is impregnated into a homogeneous medium (thin film). The magnetic anisotropy parameters of the crystallite are characterized by constant K with unit vector \mathbf{l} of the local anisotropy axis (LAA). In the chosen system of coordinates, the defect is located at the origin; the position of the vortex core is determined by radius vector ρ defined by coordinates x, y in the Cartesian system of coordinates or by the length of the radius vector and azimuthal angle φ in the cylindrical system. It should be noted that because of the small thickness of the magnet, the motion of the vortex is two-dimensional; therefore, coordinate z in the direction perpendicular to the magnet surface is not involved. The model is shown schematically in Fig. 1.

It is convenient to describe the dynamics of vortex magnetic structures in terms of collective variables; the role of such variables is played by the vortex core coordinates and velocity. With such an approach, analysis of the evolution of magnetization boils down to solving the problem of the motion of a quasiparticle, the coordinates and velocity of which are determined by the position and velocity of the magnetic vortex core. The equation for such a quasiparticle was derived by Thiele [38]:

$$\mathbf{G} \times \mathbf{v} + \hat{D}\mathbf{v} + \nabla W = 0. \quad (1)$$

Here, $\mathbf{G} = \mathbf{e}_z(2\pi\rho q M_s b/\gamma_g)(1 - \rho h)$ is the gyration vector [6, 39], M_s is the saturation magnetization, b is the magnetic film thickness, γ_g is the gyromagnetic ratio, $h = H/\mu_0 M_s$ is the dimensionless magnetic field component perpendicular to the film surface, \mathbf{e}_z is the unit vector of the z axis, \mathbf{v} is the velocity of the core, W

is the potential energy of the magnetic vortex, which contains the magnetic anisotropy energy of the crystallite, and \hat{D} is the tensor of the effective coefficients of the friction force acting on the core as on a quasiparticle in the case of damping [40–42].

The symmetry of the problem is nearly cylindrical; therefore, we will continue the description of motion of the core in the cylindrical system of coordinates. For the core velocity, we can write

$$\mathbf{v} = \mathbf{e}_\rho \frac{d\rho}{dt} + \mathbf{e}_\varphi \rho \frac{d\varphi}{dt}, \quad (2)$$

where \mathbf{e}_ρ and \mathbf{e}_φ are the unit vectors of the cylindrical system of coordinates. This gives the following expressions for the terms in Eq. (1) containing the core velocity:

$$\mathbf{G} \times \mathbf{v} = -\mathbf{e}_\rho G \rho \frac{d\varphi}{dt} + \mathbf{e}_\varphi G \frac{d\rho}{dt}, \quad (3)$$

$$\hat{D}\mathbf{v} = \begin{pmatrix} D & 0 & 0 \\ 0 & D & 0 \\ 0 & 0 & D \end{pmatrix} \begin{pmatrix} \mathbf{e}_\rho \frac{d\rho}{dt} \\ \mathbf{e}_\varphi \rho \frac{d\varphi}{dt} \\ 0 \end{pmatrix} = \mathbf{e}_\rho D \frac{d\rho}{dt} + \mathbf{e}_\varphi D \rho \frac{d\varphi}{dt}. \quad (4)$$

With account for these expressions, we can write vector equation (1) in the components:

$$\begin{aligned} -G\rho \frac{d\varphi}{dt} + D \frac{d\rho}{dt} - f_\rho &= 0, \\ G \frac{d\rho}{dt} + D\rho \frac{d\varphi}{dt} - f_\varphi &= 0. \end{aligned} \quad (5)$$

Here, the following notation has been introduced:

$$\begin{aligned} f_\rho &= -(\nabla W)_\rho = -\frac{\partial W}{\partial \rho}, \\ f_\varphi &= -(\nabla W)_\varphi = -\frac{1}{\rho} \frac{\partial W}{\partial \varphi}. \end{aligned} \quad (6)$$

We can transform system of equations (5) to

$$\begin{aligned} \frac{d\rho}{dt} &= \frac{1}{G^2 + D^2} (Df_\rho + Gf_\varphi), \\ \rho \frac{d\varphi}{dt} &= \frac{1}{G^2 + D^2} (-Gf_\rho + Df_\varphi). \end{aligned} \quad (7)$$

The solution of this system makes it possible to describe the trajectory of the vortex core.

To continue the solution, we must specify the functional form for force components f_ρ and f_φ . For this purpose, we consider the expression for energy W using the popular model of “rigid” vortex [43–45]. In the approximation of this model, we assume that the vortex distribution of magnetization is not noticeably distorted at the defect and in its neighborhood; i.e., the profile of the ansatz describing the vortex remains

unchanged during its motion and does not depend on the distance between the defect and the core.

Let us suppose that the magnetization direction is determined by unit vector $\mathbf{m}(\rho, \varphi)$, while the magnetization component perpendicular to the film surface has form $m_z(\rho, \varphi)$. Because of the small thickness of the film, vector \mathbf{m} is independent of coordinate z . The components of the magnetization vector and the vector of the local anisotropy axis can be written as

$$\begin{aligned} m_x &= q\sqrt{1 - m_z^2(\rho, \varphi)} \sin \varphi, \\ m_y &= -q\sqrt{1 - m_z^2(\rho, \varphi)} \cos \varphi, \\ l_z &= \cos \alpha, \\ l_x &= \sin \alpha \cos \gamma, \\ l_y &= \sin \alpha \sin \gamma. \end{aligned} \quad (8)$$

Here, α and γ are the polar and azimuthal angles determining the direction of the crystallite anisotropy axis (angle α is measured from the z axis).

We write the magnetic energy in form

$$W = \frac{\kappa \rho^2}{2} - KV(\mathbf{m} \cdot \mathbf{l})^2. \quad (9)$$

Here, the second term is the magnetic anisotropy energy, while the first term is the quasi-elastic energy with rigidity coefficient κ , which ensures the axially symmetric force acting on the vortex core in the direction towards the coordinate origin. This energy can be associated with the shape of the magnet (e.g., circular nanodisks with the vortex structure of magnetization [46, 47]). In addition, the implanted crystallite can distort the structure around it because of emerging mechanical stresses. This may lead to the dependence of the magnetic energy on the distance to the origin. Considering adopted notation (8), we can write energy in form

$$\begin{aligned} W &= \frac{\kappa \rho^2}{2} \\ &- KV(q\sqrt{1 - m_z^2} \sin \alpha \sin(\varphi - \gamma) + m_z \cos \alpha)^2. \end{aligned} \quad (10)$$

It is expedient to test the system of equations for the particular case of an isotropic magnet (free of defects) in the form of a thin circular disk. In this case, expression (9) for the energy contains only one first term. Then system of equations (7) takes form

$$\begin{aligned} \frac{d\rho}{dt} &= -\frac{D\kappa}{G^2 + D^2} \rho, \\ \frac{d\varphi}{dt} &= \frac{G\kappa}{G^2 + D^2}. \end{aligned} \quad (11)$$

The solutions to this system are well known (see, for example, [6]). In this case, the time dependence of the length of the radius vector has form

$$\rho(t) = \rho_0 \exp\left(-\frac{D\kappa}{G^2 + D^2} t\right), \quad (12)$$

where ρ_0 is the initial distance between the core and the disk center. The angular velocity of the vortex core moving around the disk center is given by

$$\omega = \frac{d\varphi}{dt} = \frac{G\kappa}{G^2 + D^2}. \tag{13}$$

In this case, the trajectory of the vortex is a helix converging to the origin.

The solution of system of equations (7) in general form with allowance for expression (10) is difficult. For this reason, we will consider below some interesting particular cases.

3. DEFECT WITH THE ANISOTROPY AXIS PERPENDICULAR TO THE PLANE OF THE FILM

In this section, we consider the case when the anisotropy axis is oriented along the normal to the magnet surface ($\alpha = 0$). In this case, the system is axisymmetric, i.e., energy (10) is independent of azimuthal angle φ ($f_\varphi = 0$). We can now write the force as

$$f_\rho = -\kappa\rho + KV \frac{\partial m_z^2}{\partial \rho}.$$

Then system of equations (7) takes form

$$\begin{aligned} \frac{d\rho}{dt} &= \frac{-D}{G^2 + D^2} \left(\kappa\rho - KV \frac{\partial m_z^2}{\partial \rho} \right), \\ \rho \frac{d\varphi}{dt} &= \frac{G}{G^2 + D^2} \left(\kappa\rho - KV \frac{\partial m_z^2}{\partial \rho} \right). \end{aligned} \tag{14}$$

Dividing the first equation by the second one, we obtain the following equation for the core trajectory:

$$\frac{1}{\rho} \frac{d\rho}{d\varphi} = -\frac{D}{G}. \tag{15}$$

The solution to this equation is function

$$\rho(\varphi) = \rho_0 \exp\left(\frac{D}{G}(\varphi_0 - \varphi)\right). \tag{16}$$

Here, φ_0 is the initial azimuthal angle determining the position of the vortex core.

For further estimates, we must choose the specific functional form describing the magnetization distribution in the vortex. In earlier publications, various versions of profiles were proposed [45, 46, 48–50]. We will henceforth assume that the magnetization profile is described by a function of form [51]

$$m_z = p \exp(-\rho^2/r_0^2). \tag{17}$$

Here, r_0 is the characteristic linear size of the core. Polarity p indicates the direction of the magnetization at the core center relative to the z axis. Calculations and observations show that r_0 is in the order of 10 nm. With account for expressions (16) and (17), system (14) is transformed into two independent differential

equations with separable variables, the solution to which can be represented by integrals

$$\int_{\rho_0}^{\rho} \frac{d\rho}{\rho(1 + \Lambda \exp(-2(\rho/r_0)^2))} = -\delta t, \tag{18}$$

$$\int_{\varphi_0}^{\varphi} \frac{d\varphi}{1 + \Lambda \exp(-2(\rho/r_0)^2) \exp(2\eta(\varphi_0 - \varphi))} = \omega t. \tag{19}$$

Here, the following notation has been introduced:

$$\Lambda = \frac{4KV}{\kappa r_0^2}, \quad \delta = \frac{D\kappa}{G^2 + D^2}, \quad \omega = \frac{G\kappa}{G^2 + D^2}, \quad \eta = \frac{D}{G}.$$

Characteristic dependences $\rho(t)$ and $\varphi(t)$ are shown in Fig. 2. The curves in this figure are plotted for $qp > 0$. When $qp < 0$, the $\rho(t)$ and $\varphi(t)$ dependences remain unchanged; only the direction of rotation of the core around the origin is reversed. It can be seen from the figure that for $\rho \approx r_0$, the functional time dependences of the azimuthal angle and the length of the radius vector change. This can be seen most clearly from the $\rho(t)$ curve on the semi-logarithmic scale (Fig. 3). To a high degree of accuracy, the $\rho(t)$ dependence can apparently be treated as exponential. The change to a faster $\rho(t)$ dependence is associated with the maximal approach of the vortex core to the defect. In fact, this indicates a change in the ratio of the contributions to the resultant force acting on the core due to the anisotropy energy and the energy of the core in the centrosymmetric potential. Indeed, for a large distance between the core and the origin ($\rho \gg r_0$), the exponential functions in the denominators of the integrands in relations (18) and (19) can be ignored. The calculation of these expressions gives aforementioned results (12) and (13). This should be for a large distance between the core and the defect, when the influence of the latter can be ignored.

In the opposite case of a small distance between the core and the defect, the main contribution to the energy of the system comes from the energy of interaction between the vortex and the crystallite (magnetic anisotropy energy). For distance ρ close to zero, the calculation of expressions (18) and (19) gives the following dependences:

$$\rho(t) = \rho_0 \exp(-\Lambda\delta t), \quad \varphi(t) = \varphi_0 + \Lambda\omega t. \tag{20}$$

Therefore, the velocity at which the core approaching the defect and the angular velocity of the core increase by Λ times. The change in the type of motion of the magnetic vortex can clearly be seen from the curves describing the time dependence of the core coordinates in the Cartesian system (Fig. 4). To obtain these dependences, we solved Eq. (1) numerically. Figure 4b corresponds the instant when the period of revolution of the core decreases sharply and then remains almost unchanged. The envelope of these curves illustrates qualitatively the singularity that has already been considered in the case depicted in Fig. 2.

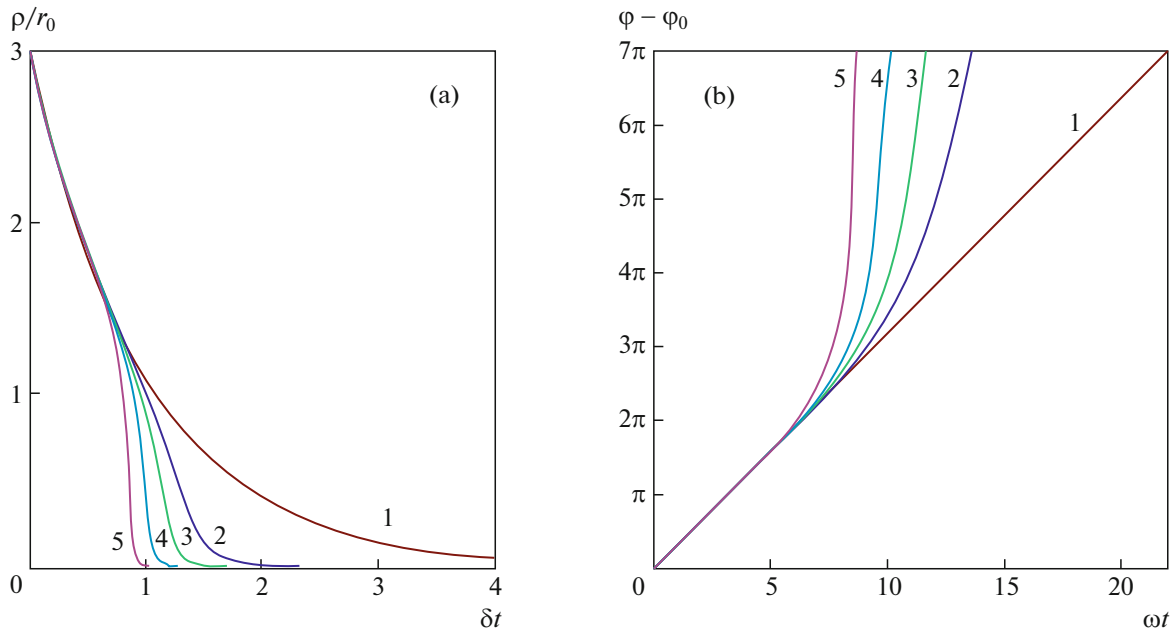


Fig. 2. Graphic representation of solutions (18) and (19) ((a) and (b), respectively). Numbers on the curves correspond to different values of parameter Λ : $\Lambda_1 = 0$, $\Lambda_2 = 5$, $\Lambda_3 = 10$, $\Lambda_4 = 20$, and $\Lambda_5 = 40$. All curves are plotted for the initial dimensionless length of radius vector $\rho_0/r_0 = 3$ and for $\eta = 0.1$.

The distance between the core and the defect at which the regimes of motion of the core change can be estimated using the simple relation following from the denominator of the integrand of expression (18):

$$\Lambda \exp(-2(\rho/r_0)^2) \approx 1, \Rightarrow \rho_c \approx r_0 \sqrt{\ln(\sqrt{\Lambda})}. \quad (21)$$

It should be noted that the dependence of ρ_c on parameter Λ is extremely slow.

It follows from previous considerations that this effect of the change in the rate of variation of dependences $\rho(t)$ and $\varphi(t)$ is characteristic of not only the chosen profile of ansatz (17). This property is also inherent in a vortex in which the magnetization distribution is described by any localized function on interval ρ_0 .

In the absence of the term responsible for centrosymmetric factor ($\kappa = 0$) in the energy of the magnet, the solution to the first equation in system (14) can be written in form

$$\text{Ei} \left(-2 \left(\frac{\rho}{r_0} \right)^2 \right) = \text{Ei} \left(-2 \left(\frac{\rho_0}{r_0} \right)^2 \right) + \delta_K t. \quad (22)$$

An analogous expression can be obtained for the azimuthal angle:

$$\begin{aligned} & \text{Ei} \left(-2 \left(\frac{\rho}{r_0} \right)^2 \exp(2\eta(\phi - \phi_0)) \right) \\ &= \text{Ei} \left(-2 \left(\frac{\rho_0}{r_0} \right)^2 \right) + \delta_K t. \end{aligned} \quad (23)$$

Here, we have introduced the following notation:

$$\delta_K = \frac{8DKV}{r_0^2(G^2 + D^2)}.$$

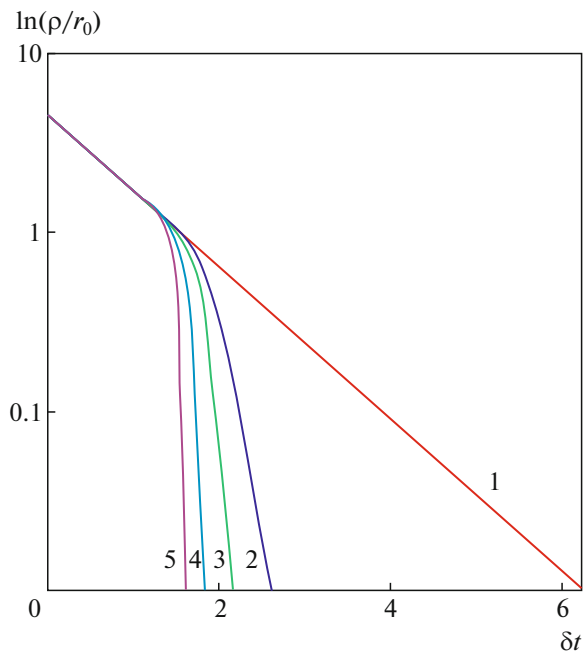


Fig. 3. Graphic representation of solution (18) on the semi-logarithmic scale. Numbers on the curves and parameters Λ , η , and ρ_0/r_0 corresponds to the numeration and parameters in Fig. 2.

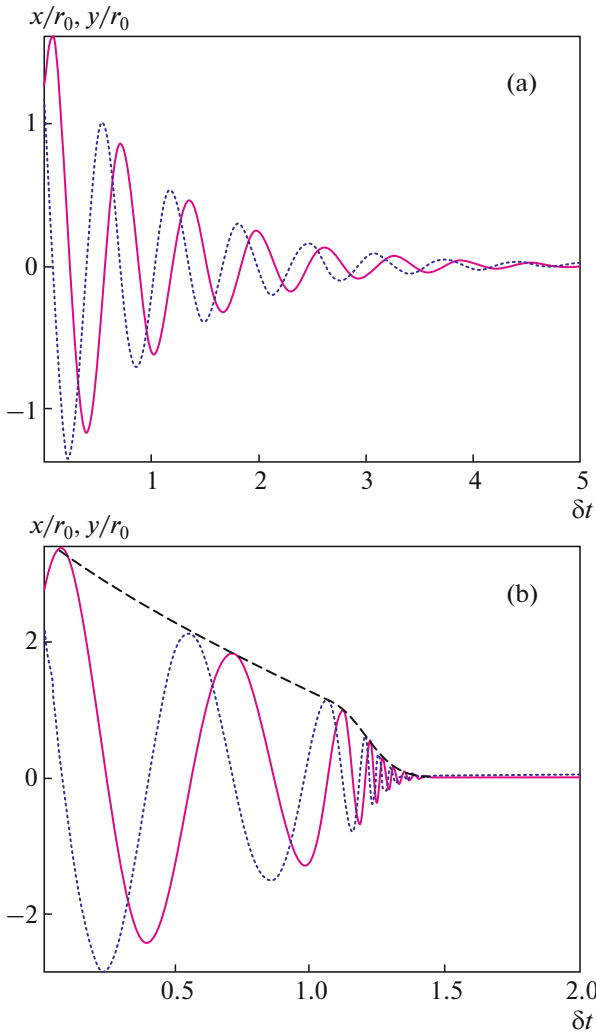


Fig. 4. Time dependences of the Cartesian coordinates of the vortex core. Solid and dashed curves describe the $x(t)$ and $y(t)$ dependences, respectively. Curves in (a) and (b) are plotted for parameters $\Lambda = 0$, $\eta = 0.1$ and $\Lambda = 1$, $\eta = 0.1$, respectively. Dashed curve in (b) is the envelope of the amplitude of displacement of the magnetic vortex core along the x axis.

The curves describing dependences (22) and (23) are shown in Fig. 5. It is interesting to note that the rotation of the core around the attracting center with a constant angular velocity is stabilized only when the defect is “trapped” by the core (i.e., for $\rho/r_0 < 1$).

We have considered above the case of the implanted defect (crystallite) with bidirectional magnetic anisotropy. It would be interesting to analyze the motion of a magnetic vortex in the presence of a defect with unidirectional anisotropy. In particular, this version is possible when an antiferromagnetic inclusion is implanted into a ferromagnetic matrix. In this case, we can write the following expression for the magnetic vortex energy:

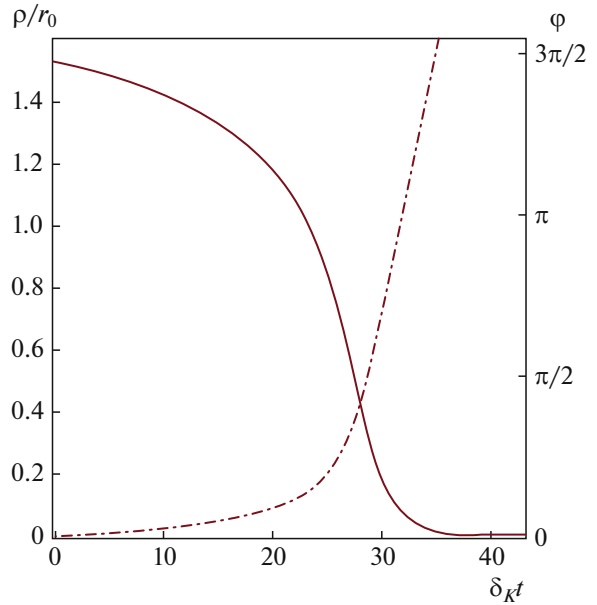


Fig. 5. Characteristic time dependences of the length of the core radius vector (solid curve) and of the azimuthal angle (dot-and-dash curve) for $\kappa = 0$.

$$W = \frac{\kappa \rho^2}{2} - KV \mathbf{m} \cdot \mathbf{l}. \tag{24}$$

Then system of equations (7) with account for expressions (17) and (24) takes form

$$\begin{aligned} \frac{d\rho}{dt} &= \frac{-D\rho}{G^2 + D^2} \left[\kappa + \frac{2\rho KV}{r_0^2} \exp\left(-\left(\frac{\rho}{r_0}\right)\right) \right], \\ \frac{d\phi}{dt} &= \frac{G}{G^2 + D^2} \left[\kappa + \frac{2\rho KV}{r_0^2} \exp\left(-\left(\frac{\rho}{r_0}\right)\right) \right]. \end{aligned} \tag{25}$$

The equation for trajectories $\rho(\phi)$ coincides with Eq. (16).

It is important to note in this connection that in contrast to the defect with bidirectional anisotropy, the right-hand sides of equations in system (25) in this case can vanish and even reverse their sign. This is possible for opposite orientations of the unidirectional anisotropy axis of the crystallite and of the vortex core polarity. Naturally, this affects the trajectory of motion of the core. Analogously to expressions (18) and (19), the solution to this system can be written in form

$$\int_{\rho_0}^{\rho} \frac{d\rho}{\rho \left(1 + \frac{1}{2} p \Lambda \exp\left(-\left(\frac{\rho}{\rho_0}\right)^2\right) \right)} = -\delta t, \tag{26}$$

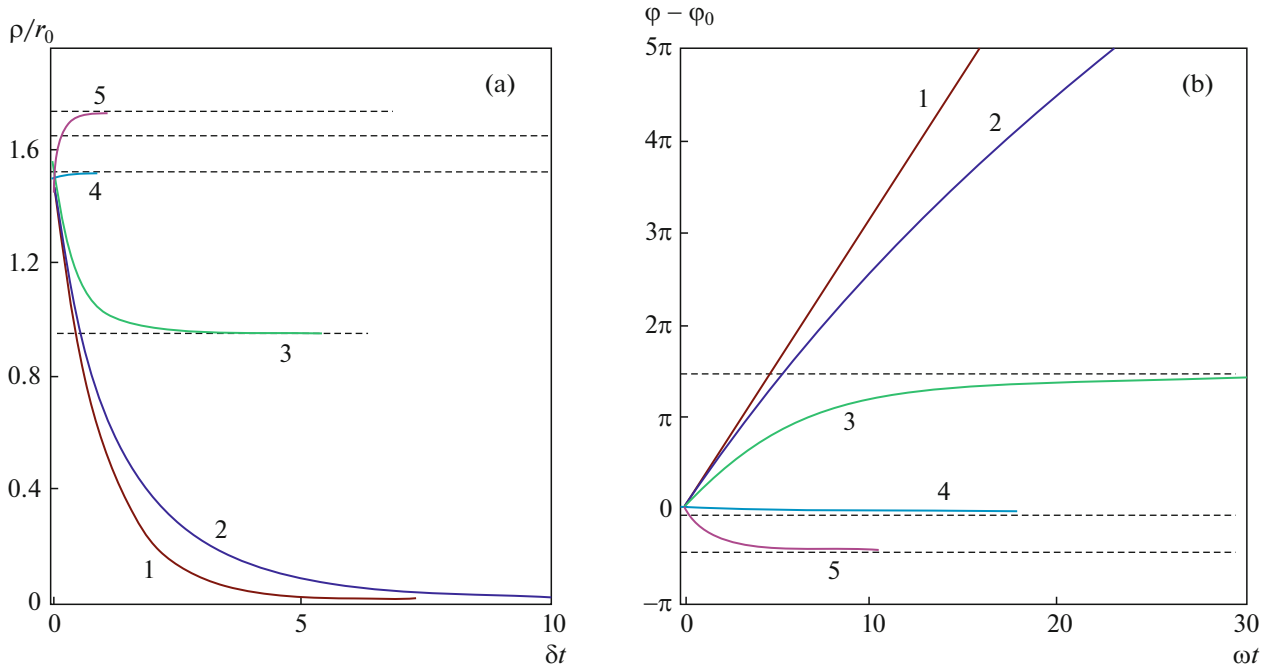


Fig. 6. Graphic representation of solutions (26) and (27) ((a) and (b), respectively). Numbers on the curves correspond to different values of parameter Λ : $\Lambda_1 = 0$, $\Lambda_2 = 1$, $\Lambda_3 = 5$, $\Lambda_4 = 20$, and $\Lambda_5 = 40$. All curves are plotted for the initial dimensionless length of radius vector $\rho_0/r_0 = 1.5$ and for $\eta = 0.1$.

$$\int_{\varphi_0}^{\varphi} \frac{d\varphi}{1 + \frac{1}{2} p \Lambda \exp\left(-\left(\frac{\rho}{r_0}\right)^2 \exp(2\eta(\varphi_0 - \varphi))\right)} = \omega t. \quad (27)$$

When the directions of the anisotropy axis and of the magnetization coincide, the behavior of the system at the center of the core does not differ from the case with bidirectional anisotropy, and dependences $\rho(t)$ and $\varphi(t)$ are similar to the curves shown in Figs. 2–5. For the opposite directions of the LAA of the crystallite and of the core polarity (e.g., $\alpha = 0$, $p = -1$ or $\alpha = \pi$, $p = +1$), the motion of the core has peculiarities associated with the divergence of the integrands in expressions (26) and (27).

Figure 6 shows several characteristic dependences $\rho(t)$ and $\varphi(t)$ obtained from the results of calculations of expressions (26) and (27) for $p = -1$. It can be seen that for certain values of Λ , there exists a certain equilibrium distance ρ_s , upon the attainment of which the motion of the vortex gradually decays. The core strives to be localized at distance ρ_s irrespective of initial position ρ_0 . The expression for calculating parameter ρ_s can easily be obtained by equating the denominator in expression (26) to zero. This gives

$$\rho_s = r_0 \sqrt{\ln \frac{\Lambda}{2}}. \quad (28)$$

It should be noted that for $\Lambda \leq 2$, the equilibrium position of the core is at the coordinate origin, i.e., directly on the defect ($\rho_s = 0$).

Figure 7 shows the time dependences of the coordinates in the Cartesian system and the corresponding trajectories of the core in the case considered here, which were obtained from the numerical solution of system of equations (7). Therefore, in the presence of a defect with a unidirectional anisotropy axis perpendicular to the film surface, the “capture” of the core by the defect can be realized so that the core center is at a certain distance from the crystallite, but not on the defect itself as in the case of bidirectional anisotropy.

4. DEFECT WITH THE ANISOTROPY AXIS LYING IN THE PLANE OF THE FILM

In this section, we consider the scenario of motion of a magnetic vortex in the field of a defect with the anisotropy axis lying in the plane of the magnet ($\alpha = \pi/2$, $\gamma = 0$). In this case, the potential is not centrosymmetric and depends on the azimuthal angle of vortex core l . We first analyze the simple case when the total energy does not contain the centrosymmetric term (i.e., we set $\kappa = 0$). Then we obtain the following expressions for energy and forces:

$$W = -KV(1 - m_z^2) \sin^2 \varphi. \quad (29)$$

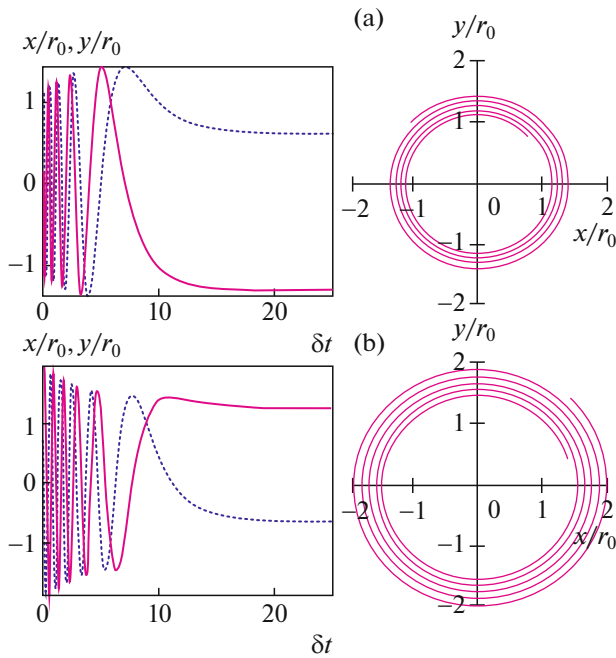


Fig. 7. Time dependences of the Cartesian coordinates of the vortex core in the model of unidirectional anisotropy of the crystallite. Solid and dotted curves describe the $x(t)$ and $y(t)$ dependences, respectively. The curves are plotted for $\Lambda = 1, p = -1, \eta = 0.01, \rho_0/r_0 = 1.1$ (a) and 2 (b).

$$\begin{aligned}
 f_\rho &= KV \frac{dm_z^2}{d\rho} \sin^2 \varphi, \\
 f_\varphi &= \frac{1}{\rho} KV(1 - m_z^2) \sin 2\varphi.
 \end{aligned}
 \tag{30}$$

System of equations (7) takes form

$$\begin{aligned}
 \frac{d\rho}{dt} &= \frac{KV}{G^2 + D^2} \left(\frac{1}{\rho} G(1 - m_z^2) \sin 2\varphi \right. \\
 &\quad \left. + D \frac{d(1 - m_z^2)}{d\rho} \sin^2 \varphi \right), \\
 \rho \frac{d\varphi}{dt} &= \frac{KV}{G^2 + D^2} \left(\frac{1}{\rho} D(1 - m_z^2) \sin 2\varphi \right. \\
 &\quad \left. - G \frac{d(1 - m_z^2)}{d\rho} \sin^2 \varphi \right).
 \end{aligned}
 \tag{31}$$

We obtain the differential equation for the core trajectory by dividing the first equation in system (31) by the second equation:

$$\frac{d\rho}{d\varphi} = \frac{2 \cot \varphi + \eta \xi(\varphi)}{2\eta \cot \varphi - \xi(\varphi)}.
 \tag{32}$$

Here, we have used the following notation:

$$\varrho = \ln \frac{\rho}{\rho_0}, \quad \xi(\varrho) = \frac{d \ln(1 - m_z^2)}{d\varrho}.$$

In the absence of damping ($\eta = 0$), this equation holds for function

$$m_z(\rho) = 1 - (1 - m_z^2(\rho_0)) \left(\frac{\sin \varphi_0}{\sin \varphi} \right)^2.
 \tag{33}$$

As before, parameters ρ_0 and φ_0 specify the initial position of the core and $m_z(\rho)$ are arbitrary functions describing the magnetization profile of the core (which are not necessarily defined by expression (17)) and calculated in the corresponding coordinates.

For $\kappa = 0$, the minimal value of the energy of the system is realized when magnetization vector \mathbf{m} is collinear to vector \mathbf{l} of the anisotropy axis of the defect. This state obviously corresponds to the maximal distance between the core and the crystallite ($\rho \rightarrow \infty$); i.e., the vortex is repelled by the defect. Since functions $m_z(\rho)$ are localize in a small region near r_0 , the value of $m_z \rightarrow 0$ for $\rho \rightarrow \infty$. Using relation (33), we can determined the direction of motion of the vortex core (azimuthal angle φ_∞). To this end, we equate the left-hand side of Eq. (33) to zero, which gives

$$\sin \varphi_\infty = \pm \sqrt{1 - m_z^2(\rho_0)} \sin \varphi_0.
 \tag{34}$$

It is interesting to note that a noticeably curvilinear motion of the core could be observed only near the defect. For a large distance from the crystallite ($m_z(\rho) \ll 1$), the azimuthal angle remains unchanged, and the motion of the vortex is translational in the direction away from the crystallite like the motion of a particle repelled from the defect. In spite of the absence of axial symmetry in the field produced by the defect, the core moves along the radius vector. This is obviously due to the complex influence of the asymmetric potential and the gyrotropic effect associated with magnetization precession during the motion of the vortex. Figure 8 shows the trajectories of the magnetic vortex core for zero damping tensor \hat{D} , which were obtained from numerical solution of equation of motion (1) in the Cartesian coordinates.

To find the time dependence of the position of the vortex core, we return to system of equations (31). When $\rho_0/r_0 \geq 1$, the first equation can be written approximately in form

$$\frac{d\rho}{dt} = \frac{KV}{\rho G} \sin 2\varphi,
 \tag{35}$$

where angle φ is defined by expression (34). The solution to this equation is function

$$\rho(t) = \sqrt{\rho_0^2 + \frac{2}{G} KV \sin(2\varphi_\infty)t}.
 \tag{36}$$

The dependence of the distance from the vortex center to the repelling center described by law $\rho^2 \propto t$ indicates that at a large distance, the core as a quasi-particle is in the effective potential of the defect, which varies in accordance with law $W_{\text{eff}} \propto 1/\rho^2$. Indeed, the

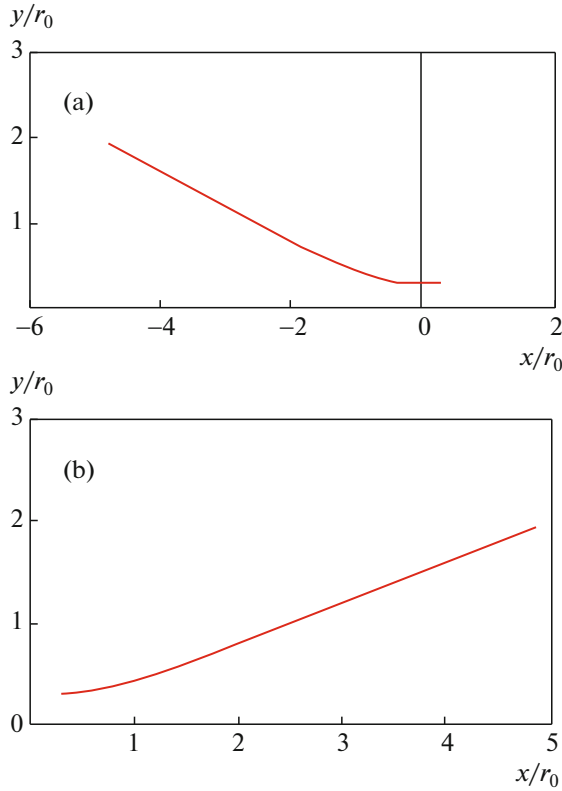


Fig. 8. Trajectories of motion of the magnetic vortex core without damping for $pq < 0$ (a) and $pq > 0$ (b). Both curves are plotted for initial conditions $\rho_0/r_0 = 0.4$ and $\varphi_0 = \pi/4$.

solution of the simple problem in mechanics with account for expression (36) gives

$$W_{\text{eff}} = \frac{1}{2} \mu \left(\frac{KV \sin \varphi_\infty}{\rho G} \right)^2. \quad (37)$$

Here, μ is the effective mass of the vortex as a quasiparticle.

With account for equation (33) of the trajectory, we obtain the following differential equation with separable variables for the second equation in system (31):

$$\frac{d\varphi}{dt} = -\frac{KV}{Gr_0^2} (\sin^2 \varphi - \sin^2 \varphi_\infty). \quad (38)$$

The solution to this equation is function

$$\tan \varphi = \tan(\varphi_\infty) \tanh \left(\operatorname{arctanh} \left(\frac{\tan \varphi_0}{\tan \varphi_\infty} \right) + \frac{4KV \sin 2\varphi_\infty t}{Gr_0^2} \right). \quad (39)$$

In the case of damping, it is difficult to obtain the general solution to Eq. (32). For this reason, we confine our analysis to the case when $\rho_0/r_0 \geq 1$. In this approximation, $\xi(\rho) \ll 1$, and Eq. (32) takes the following simple form:

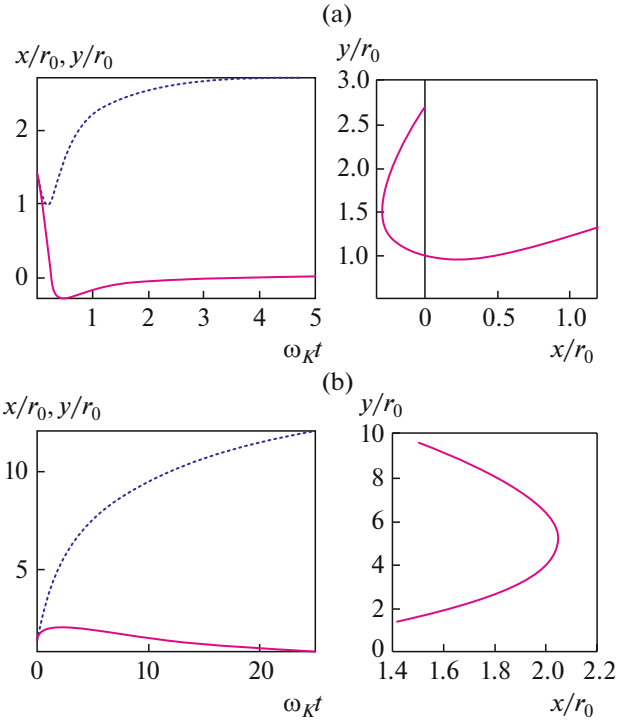


Fig. 9. Characteristic shapes of trajectories for $\alpha = \pi/2$, $\eta = 0.4$, $\rho_0/r_0 = 2$, $\varphi_0 = \pi/4$, and $\kappa = 0$ from the results of solution of system of equations (31) for $qp < 0$ (a) and $qp > 0$ (b). Solid and dotted curves show dependences $x(t)$ and $y(t)$, respectively.

$$\frac{d\rho}{d\varphi} = \frac{1}{\eta}. \quad (40)$$

The solution to this equation is dependence

$$\rho(\varphi) = \rho_0 \exp \left(\frac{G}{D} (\varphi - \varphi_0) \right). \quad (41)$$

With account for this relation, the second equation in system (31) has solution

$$\int_{\varphi_0}^{\varphi} \frac{\exp \left(\frac{2}{\eta} (\varphi - \varphi_0) \right)}{\sin 2\varphi} d\varphi = \frac{1}{8} \left(\frac{r_0}{\rho_0} \right)^2 \delta_K t. \quad (42)$$

Analogously, for the time dependence of the distance between the core and the crystallite, we obtain

$$\int_{\rho_0}^{\rho} \frac{\rho d\rho}{\sin(2\varphi_0 + 2\eta \ln(\rho/\rho_0))} = r_0^2 \omega_K t. \quad (43)$$

Here, $\omega_K = GKV/(G^2 + D^2)$. The trajectories of vortex cores are shown in Fig. 9. It should be noted that damping leads to the rapid orientation of the radius vector of the core in the direction perpendicular to the local anisotropy axis of the crystallite. This direction corresponds to decreasing anisotropy energy (see Fig. 1).

5. DISCUSSION

Analysis of the interaction of a magnetic vortex with a defect (crystallite) simulated by a magnetic anisotropy nonuniformity has revealed a diversity of scenarios for behavior of the magnetization. When the magnetic anisotropy axis of the defect (crystallite) does not lie in the plane of the magnet, the field of the defect “traps” the vortex. If the defect has bidirectional anisotropy, the vortex core as a quasiparticle strives to be located directly on the defect. If the potential in which the core moves is produced not only by the field of the defect, but also by an axisymmetric field of a different origin, an interesting clearly manifested effect of the change in regimes of motion of the vortex is observed, which differ in the frequency of rotation of the core around the crystallite and in the laws of variation of the distance to the defect with time. An additional axisymmetric potential can exist, for example, because of the limited size of the magnet (magnetostatic potential) or due to mechanical stresses near the crystallite (magnetoelastic potential). This circumstance can be extremely important in designing devices for the control over the motion of magnetic vortices and skyrmions (e.g., for bringing a vortex to the resonant state). It is important to note that the effect of the change in the angular velocity of rotation of the vortex around the defect is observed for any profile describing the magnetization distribution in the core. It is only required that function m_z describing this distribution be localized in a small region near r_0 . Such an effect was observed in experiment [35].

In the case when the defect (crystallite) is characterized by unidirectional magnetic anisotropy, the vortex core can experience both attraction and repulsion depending on the mutual directions of the anisotropy axes of the crystallites and the polarity of the vortex. Because of the competition between the centrosymmetric attractive parabolic potential and the repulsive potential due to anisotropy, there exists an equilibrium distance between the core and the defect (see expression (28)). The existence of multiple local minima of the skyrmion (vortex) energy near the defect was observed in experiment [34].

The behavior of a magnetic vortex in the field of a defect with the anisotropy axis lying in the plane of the magnet is equally interesting. In this case, the anisotropy energy ensures the repulsion of the vortex core from the defect; for extremely low damping, the core moves almost in straight line from the crystallite in accordance with the law corresponding to effective potential energy $W_{\text{eff}} \propto \rho^{-2}$. This is observed precisely for the magnetization nonuniformity in the form of a magnetic vortex, i.e., the object (quasiparticle) that experiences the action of the gyroscopic force during its motion. We explain the radial motion of the core in the direction from the defect (reflection of the vortex from the defect) by the competition between two fac-

tors: the gyroscopic effect and the moment of forces produced by anisotropy of the crystallite.

The gyroscopic effect is manifested the more clearly the higher the core velocity. Therefore, in the presence of appreciable damping, the moment of forces associated with anisotropy of the defect becomes prevailing upon a decrease in the velocity of the vortex. In this case, the trajectory of the core is curvilinear, and the equilibrium position corresponds to the direction of the radius vector, which is perpendicular to the anisotropy axis of the crystallite (which corresponds to the anisotropy energy minimum).

6. CONCLUSIONS

Thus, we can state that such objects as magnetic vortices in the vicinity of inhomogeneities of the magnetic structure demonstrate a diversified behavior (“capture” of a vortex by a defect with a clearly manifested change in the frequency of rotation, reflection from the defect with different trajectories of motion, etc.). This necessitates the account for the peculiarities of the interaction of vortex cores with defects present in magnets. This is especially important in designing spintronics devices for various purposes.

FUNDING

This study was supported by the Russian Foundation for Basic Research (project no. 18-02-00161).

REFERENCES

1. D. A. Allwood, G. Xiong, C. C. Faulkner, D. Atkinson, D. Petit, and R. P. Cowburn, *Science* (Washington, DC, U. S.) **309**, 1688 (2005).
2. M. Hayashi, L. Thomas, R. Moriya, Ch. Rettner, and S. S. P. Parkin, *Science* (Washington, DC, U. S.) **320**, 209 (2008).
3. S. S. P. Parkin, M. Hayashi, and L. Thomas, *Science* (Washington, DC, U. S.) **320**, 190 (2008).
4. W. Kang, Y. Huang, Ch. Zheng, W. Lv, N. Lei, Y. Zhang, X. Zhang, Y. Zhou, and W. Zhao, *Sci. Rep.* **6**, 23164 (2016).
5. A. S. Mel’nikov, A. V. Samokhvalov, and V. L. Vadi-mov, *JETP Lett.* **102**, 775 (2015).
6. J. Kim and S.-B. Choe, *J. Magn.* **12**, 113 (2007).
7. A. Puzic, B. van Waeyenberge, K. W. Chou, P. Fischer, H. Stoll, G. Schutz, T. Tylliszczak, K. Rott, H. Bruckl, G. Reiss, I. Neudecker, Th. Haug, M. Buess, and C. H. Back, *J. Appl. Phys.* **97**, 10E704 (2005).
8. B. Pigeau, G. de Loubens, O. Klein, A. Riegler, F. Lochner, G. Schmidt, L. W. Molenkamp, V. S. Tiberkevich, and A. N. Slavin, *Appl. Phys. Lett.* **96**, 132506 (2010).
9. K. Yu. Guslienko, V. Novosad, Y. Otani, H. Shima, and K. Fukamichi, *Phys. Rev. B* **65**, 024414 (2001).
10. A. K. Zvezdin and K. A. Zvezdin, *J. Low Temp. Phys.* **36**, 826 (2010).

11. S. V. Stepanov, A. E. Ekomasov, A. K. Zvezdin, and E. G. Ekomasov, *Phys. Solid State* **60**, 1055 (2018).
12. V. A. Orlov, R. Yu. Rudenko, A. V. Kobayakov, A. V. Lukyanenko, P. D. Kim, V. S. Prokopenko, and I. N. Orlova, *J. Exp. Theor. Phys.* **126**, 523 (2018).
13. J. C. Martinez and M. B. A. Jalil, *New J. Phys.* **18**, 033008 (2016).
14. L. Gonzalez-Gomez, J. Castell-Queralt, N. Del-Valle, A. Sanchez, and C. Navau, *Phys. Rev. B* **100**, 054440 (2019).
15. X. Liang, G. Zhao, L. Shen, J. Xia, Li Zhao, X. Zhang, and Y. Zhou, *Phys. Rev. B* **100**, 144439 (2019).
16. X. Gong, H. Y. Yuan, and X. R. Wang, arXiv:1911.01245v1 [cond-mat.mes-hall] (2019).
17. C. Navau, N. Del-Valle, and A. Sanchez, *J. Magn. Magn. Mater.* **465**, 709 (2018).
18. H. C. Choi, S.-Z. Lin, and J.-X. Zhu, *Phys. Rev. B* **93**, 115112 (2016).
19. J. Muller and A. Rosch, *Phys. Rev. B* **91**, 054410 (2015).
20. J. A. J. Burgess, J. E. Losby, and M. R. Freeman, *J. Magn. Magn. Mater.* **361**, 140 (2014).
21. D. Stosic, T. B. Luderer, and M. V. Milosevic, *Phys. Rev. B* **96**, 214403 (2017).
22. D. Stosic, *Numerical Simulations of Magnetic Skyrmions in Atomically-thin Ferromagnetic Films* (Univ. Fed. Pernambuco, Recife, 2018).
23. J. Iwasaki, M. Mochizuki, and N. Nagaosa, *Nat. Commun.* **4**, 1463 (2012).
24. R. Brearton, M. W. Olszewski, S. Zhang, M. R. Eskildsen, C. Reichhardt, C. J. O. Reichhardt, G. van der Laan, and T. Hesjedal, *MRS Adv.* (2019). <https://doi.org/10.1557/adv.2019.43>
25. W. Legrand, D. Maccariello, N. Reyren, K. Garcia, C. Moutafis, C. Moreau-Luchaire, S. Collin, K. Bouzehouane, V. Cros, and A. Fert, *Nano Lett.* **17**, 2703 (2017).
26. J.-V. Kim and M.-W. Yoo, *Appl. Phys. Lett.* **110**, 132404 (2017).
27. C. Reichhardt, D. Ray, and C. J. Olson Reichhardt, *Phys. Rev. Lett.* **114**, 217202 (2015).
28. K. Zeissler, S. Finizio, C. Barton, A. J. Huxtable, J. Massey, J. Raabe, A. V. Sadovnikov, S. A. Nikitov, R. Brearton, T. Hesjedal, G. van der Laan, M. C. Rosamond, E. H. Linfield, G. Burnell, and C. H. Marrows, *Nat. Commun.* **11**, 428 (2020).
29. J. Castell-Queralt, L. Gonzalez-Gomez, N. Del-Valle, A. Sanchez, and C. Navau, *Nanoscale* **11**, 12589 (2019).
30. A. Salimath, A. Abbout, A. Brataas, and A. Manchon, *Phys. Rev. B* **99**, 104416 (2019).
31. J. Iwasaki, M. Mochizuki, and N. Nagaosa, *Nat. Nanotechnol.* **8**, 742 (2013).
32. H. T. Fook, W. L. Gan, and W. S. Lew, *Sci. Rep.* **6**, 21099 (2016).
33. M. Rahm, J. Biberger, V. Umansky, and D. Weiss, *J. Appl. Phys.* **93**, 7429 (2003).
34. I. L. Fernandes, J. Bouaziz, S. Blugel, and S. Lounis, *Sci. Rep.* **9**, 4395 (2018).
35. R. L. Compton and P. A. Crowell, *Phys. Rev. Lett.* **97**, 137202 (2006).
36. T. Y. Chen, M. J. Erickson, and P. A. Crowell, *Phys. Rev. Lett.* **109**, 097202 (2012).
37. C. Hanneken, *New J. Phys.* **18**, 055009 (2016).
38. A. Thiele, *Phys. Rev. Lett.* **30**, 230 (1973).
39. K. Yu. Guslienko, B. A. Ivanov, V. Novosad, Y. Otani, H. Shima, and K. Fukamichi, *J. Appl. Phys.* **91**, 8037 (2002).
40. P. D. Kim, V. A. Orlov, V. S. Prokopenko, S. S. Zamai, V. Ya. Prints, R. Yu. Rudenko, and T. V. Rudenko, *Phys. Solid State* **57**, 30 (2015).
41. D. Reitz, A. Ghosh, and O. Tchernyshyov, *Phys. Rev. B* **97**, 054424 (2018).
42. X. Zhang, J. Müller, J. Xia, M. Garst, X. Liu, and Y. Zhou, *New J. Phys.* **10**, 065001 (2017).
43. K. Yu. Guslienko, X. F. Han, D. J. Keavney, R. Divan, and S. D. Bader, *Phys. Rev. Lett.* **96**, 067205 (2006).
44. M. Wolf, U. K. Robler, and R. Schafer, *J. Magn. Magn. Mater.* **314**, 105 (2007).
45. W. Scholz, K. Yu. Guslienko, V. Novosad, D. Suess, T. Schrefl, R. W. Chantrell, and J. Fidler, *J. Magn. Magn. Mater.* **266**, 155 (2003).
46. V. A. Orlov and P. D. Kim, *J. Sib. Fed. Univ. Math. Phys.* **6**, 86 (2013).
47. V. P. Kravchuk and D. D. Sheka, *Phys. Solid State* **49**, 1923 (2007).
48. N. A. Usov and S. E. Peschany, *J. Magn. Magn. Mater.* **118**, L290 (1993).
49. A. Aharoni, *J. Appl. Phys.* **68**, 2892 (1990).
50. A. Wachowiak, J. Wiebe, M. Bode, O. Pietzsch, M. Morgenstern, and R. Wiesendanger, *Science* (Washington, DC, U. S.) **298**, 577 (2002).
51. E. Feldtkeller and H. Thomas, *Phys. Kond. Mater.* **4**, 8 (1965).

Translated by N. Wadhwa